

Carbothermic reduction of zinc sulfide in the presence of calcium oxide and lithium carbonate

Y. C. Peng · C. I. Lin · H. K. Chen

Received: 27 February 2006 / Accepted: 9 February 2007 / Published online: 30 May 2007
© Springer Science+Business Media, LLC 2007

Abstract The carbothermic reduction of zinc sulfide in the presence of calcium oxide and lithium carbonate was studied using a thermogravimetric analysis system (TGA), an X-ray diffractometer (XRD), an atomic absorption spectrometer (AAS), a carbon and sulfur determinator (CSD), an elemental analyzer (EA), a scanning electron microscope (SEM) and a surface area analyzer (SAA). Experimental results revealed that the reaction rate was significantly enhanced by the lithium carbonate catalyst. The results of TGA, AAS, CSD and EA were found to be comparable. A reaction mechanism was proposed to interpret the overall reaction.

Introduction

The carbothermic reduction of zinc sulfide in the presence of calcium oxide or calcium carbonate plays an important role in the following two processes: pyrometallurgical extraction of zinc from zinc sphalerite [1] and zinc recovery from spent zinc oxide catalyst generated from a steam reforming process [2].

In this reaction, carbon acts as a reductant to reduce zinc sulfide and calcium oxide or calcium carbonate, a scavenging agent to fix the sulfur content in zinc sulfide to prevent the emission of sulfur dioxide to atmosphere. Eight publications

on this topic can be found [1, 3–9]. To speed up the reaction, the following catalysts have been added to the solid sample: Na_2CO_3 [1, 3], Na_2SO_4 [1, 4], NaF [1] and Fe_2O_3 [1, 4].

The reaction with Na_2CO_3 or Na_2SO_4 catalyst [1, 4] has been extensively studied and mechanisms have been proposed to interpret the reaction with Na_2CO_3 catalyst. Unfortunately, the reaction with Li_2CO_3 catalyst has not been investigated.

To clarify the reaction with lithium carbonate catalyst, the carbothermic reduction of zinc sulfide in the presence of calcium oxide and lithium carbonate in an argon gas stream over the temperature 1,180–1,353 K is studied in this work. A TGA, an XRD, an AAS, a CSD and an EA are used to measure the variations in weight and composition of the solid sample during reaction. An SEM and an SAA are employed to monitor the structural changes of the sample. Moreover, a reaction mechanism is developed to interpret this reaction according to the experimental data obtained. This study may help enhance the understanding of this reaction system.

Experimental procedure

Materials

Argon with a minimum 99.995 % purity was purchased from Yuang-Ron Gas Co. (Taipei, Taiwan). Zinc sulfide (reagent grade, minimum purity of 99.99 %) and calcium oxide (reagent grade, minimum purity of 99.99 %) were procured from Cerac Chem. Co. (Milwaukee, WI, USA) while carbon black (reagent grade, minimum purity of 99.99 %) and lithium carbonate (reagent grade, minimum purity of 99 %) were supplied by Strem Chem. Co. (Newbury port, MA, USA).

Y. C. Peng · C. I. Lin (✉)
Department of Chemical Engineering, National Taiwan
University of Science and Technology, Taipei 106, Taiwan
e-mail: cilin@ch.ntust.edu.tw

H. K. Chen
Department of Biochemical Engineering, Hwa-Hsia Collage of
Technology and Commerce, Taipei 235, Taiwan

Sample preparation

Zinc sulfide, calcium oxide and lithium carbonate of average sizes of 5.98×10^{-6} , 17.9×10^{-6} and 526.4×10^{-6} m, respectively, as determined by a laser diffraction particle size analyzer (LS-230, Beckman Coulter, Miami, Florida, USA) were used; while carbon black was screened through a set of Tyler standard screens to obtain the size of 67.7×10^{-6} m. After mixing in a V-type blender (S-2, Tsutsui Scientific Instruments, Tokyo, Japan) for 21,600 s (6 h), these powders were dried at 378 K for 43,200 s (12 h) and packed in a cylindrical alumina crucible of 0.02 m diameter and 0.03 m height. The total sample weight is 4.756×10^{-4} kg and the weights of ZnS, C, CaO, and Li_2CO_3 in one solid sample are 3.552×10^{-4} , 0.265×10^{-4} , 0.927×10^{-4} , 0.012×10^{-4} kg, respectively.

Carbothermic reduction

The carbothermic reduction was conducted in a typical TGA constructed by the members of this laboratory.

The reaction tube in the TGA, without solid sample loaded, was first heated up with argon flowing through the tube. When a desired temperature was reached and maintained for 1,800 s (0.5 h), the reaction tube was opened and the crucible with solid sample of 0.4756 g was placed inside. Then, the tube was closed and the reaction started. The pressure in the TGA was held at 20–40 Pa higher than the atmospheric one. The solid sample was removed and quenched by an argon stream once the reaction time was reached.

Two series of experiments have been performed. In the first series, the temperature was kept at 1,303 K and reaction time was varied as: 0, 300, 600, 900, 1,200, 1,500, 1,800, 2,100 and 2,400 s to investigate the effect of reaction time on the variations in composition and physical properties of the solid sample. In the second series, the reaction time was maintained at 2,400 s (0.67 h) and five temperatures (1,180, 1,203, 1,253, 1,303 and 1,353 K) were employed. The relevant experimental conditions are depicted in Table 1. Unreacted and partially reacted samples were analyzed by a TGA, an XRD, an AAS, a CSD, an EA, an SEM and an SAA.

Analysis by XRD

Solid samples, unreacted and partially reacted, were ground by a pestle and a mortar to fine powders for the XRD analysis. Copper K α radiation was generated by a Rotaflex Ru-200B diffractometer (Rigaku Co., Tokyo, Japan), utilizing an acceleration voltage of 4.0×10^4 V and a current of 100 mA. A diffraction angle of 20–70 deg was scanned at a rate of 0.167 deg s $^{-1}$.

Table 1 Values of experimental variables

Variable	Value*
Argon flow rate (10^{-5} m 3 s $^{-1}$)	<u>0.50</u>
Sample height (m)	<u>0.005</u>
Sample diameter (m)	<u>0.02</u>
Sample weight (10^{-3} kg)	<u>0.4756</u>
Initial molar ratio of C/ZnS (–)	<u>2.0</u>
Initial molar ratio of CaO/ZnS (–)	<u>1.5</u>
Initial molar ratio of Li_2CO_3 /ZnS (–)	<u>0.015</u>
Average size of ZnS aggregate (10^{-6} m)	<u>5.98</u>
Size of carbon aggregate (10^{-6} m)	<u>67.7</u>
Average size of CaO (10^{-6} m)	<u>17.90</u>
Initial bulk density (kg m $^{-3}$)	<u>429.1</u>
Reaction temperature (K)	1,180, 1,203, 1,253, <u>1,303</u> , 1,353
Reaction time (s)	0, 300, 600, 900, 1,200, 1,500, 1,800, 2,100, <u>2,400</u>

*Underlined values are standard operating variables

Analysis by AAS and TGA

As mentioned before, the carbothermic reductions were carried out in a TGA, which recorded the weights of the solid sample during reaction. To check the accuracy of zinc yield calculated from the weight loss obtained from TGA, eight solid samples reacted at 1,303 K for different durations were analyzed by an AAS (AA-20, Varian Co., Mulgrave, Australia). The solid sample was pretreated as follows. It was mixed with 2×10^{-5} m 3 8 N nitric acid at 50°C for 1,200 s (0.33 h). The slurry thus produced was filtered by a piece of 5C Adventic filter paper and the filtrate was then diluted with distilled water. After that, the zinc content in the liquid sample was analyzed by the AAS, which was operated at a wavelength of 2.139×10^{-7} m, a width of light grid of 1×10^{-9} m and an electric current of 5×10^{-3} A.

Analysis by CSD and EA

A carbon and sulfur determinator (CS-244, Leco, St. Joseph, Michigan, USA) and an elemental analyzer (Vario EL, Heraeus, Germany) were employed to measure the residual content of carbon and sulfur in the solid samples.

Analysis by SEM

The appearance of the grains of zinc sulfide, carbon black, calcium oxide and lithium carbonate as well as unreacted

and reacted solid samples were observed with an SEM (S360, Cambridge, Cambridge, United Kingdom).

Analysis by SAA

The specific surface area, specific pore volume and average pore diameter of the solid sample were measured by an SAA (AS1MP-LP-VP2, Quantachrome, Boyton Beach, Florida, USA). The specific surface area was calculated according to the adsorption method of Brunauer–Emmett–Teller (BET) [10], while the specific pore volume and average pore diameter were determined by the cumulative desorption method of Barreott–Joyner–Halenda (BJH) [11]. Adsorption and desorption isotherms of nitrogen were determined gravimetrically at the temperature of liquid nitrogen. Prior to the measurement, each sample was evacuated down to 66.7 kPa at 423 K for at least 43,200 s (12 h).

Auxiliary experiments

To clarify the reaction mechanism, two kinds of auxiliary experiments were performed. The first one was to study the rates of reaction between zinc sulfide and calcium oxide. Two experimental runs were carried out under the following conditions. One was run with molar ratio of CaO/Li₂CO₃/ZnS 1.5/0.015/1.0 and the other, 1.5/0/1.0. The experiments were carried out at 1,303 K for different durations: 0, 600, 1,200, 1,800 and 2,400 s and the reacted samples were analyzed by the XRD.

The second kind of auxiliary experiments aimed to investigate the possibility of reaction between zinc sulfide and lithium carbonate. Zinc sulfide and lithium carbonate was mixed at the molar ratio of Li₂CO₃/ZnS = 1/1 and the solid sample was loaded in the flowing argon stream at 1,303 K for 2,400 s. The unreacted and reacted samples were analyzed by the XRD.

Results and discussion

Analysis of XRD

α -ZnS, β -ZnS, ZnO, CaO, CaS and Li₂CO₃ were observed in the XRD patterns of the partially reacted samples. However, peaks of C and Zn could not be seen due to the amorphous form of C and the vaporization of Zn, respectively. If 26.92, 36.25, 37.35, 31.41 and 34.10 deg were chosen as the characteristic peaks for α -ZnS, ZnO, CaO, CaS and Li₂CO₃ [12], respectively, the relationships between the peak intensities and reaction times as well as those between the peak intensities and reaction temperatures can be obtained as shown in Figs. 1 and 2, respectively. The plot of peak intensity of β -ZnS against time, however, could not be worked out since almost all peaks of

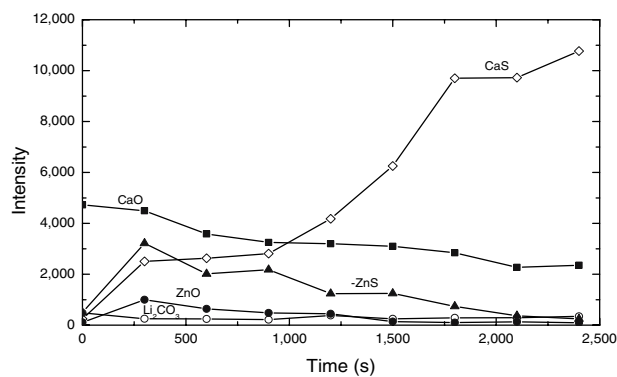


Fig. 1 Variations in the intensities of XRD peaks of α -ZnS, ZnO, CaO, CaS and Li₂CO₃ as a function of reaction time. Q , $0.50 \times 10^{-5} \text{ m}^3 \text{ s}^{-1}$; h , 0.005 m; T , 1,303 K; $N_{\text{C}}^0/N_{\text{ZnS}}^0$, 2.0; $N_{\text{CaO}}^0/N_{\text{ZnS}}^0$, 1.5; $N_{\text{Li}_2\text{CO}_3}^0/N_{\text{ZnS}}^0$, 0.015; d_{ZnS} , $5.98 \times 10^{-6} \text{ m}$; d_{C} , $67.7 \times 10^{-6} \text{ m}$; d_{CaO} , $17.90 \times 10^{-6} \text{ m}$; ρ_0 , 429.1 kg m^{-3}

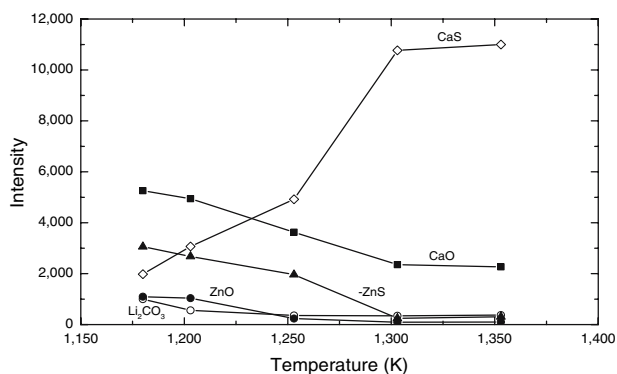


Fig. 2 Variations in the intensities of XRD peaks of α -ZnS, ZnO, CaO, CaS and Li₂CO₃ as a function of reaction temperature. Q , $0.50 \times 10^{-5} \text{ m}^3 \text{ s}^{-1}$; h , 0.005 m; $N_{\text{C}}^0/N_{\text{ZnS}}^0$, 2.0; $N_{\text{CaO}}^0/N_{\text{ZnS}}^0$, 1.5; $N_{\text{Li}_2\text{CO}_3}^0/N_{\text{ZnS}}^0$, 0.015; d_{ZnS} , $5.98 \times 10^{-6} \text{ m}$; d_{C} , $67.7 \times 10^{-6} \text{ m}$; d_{CaO} , $17.90 \times 10^{-6} \text{ m}$; ρ_0 , 429.1 kg m^{-3} ; t , 2,400 s

β -ZnS overlap with those of other components. The variation in amount of a specific substance in the solid sample can be obtained from the change in intensity of that species as shown in Figs. 1 and 2, since the amount of that species is qualitatively proportional to its peak intensity.

The trends of the variations in α -ZnS, ZnO, CaO and CaS of the Li₂CO₃ catalyzed reaction shown in Figs. 1 and 2 are very close to those of the uncatalyzed reaction [8]. The only difference is that the time for the reaction to cease has been greatly reduced from 10,800 s to 2,400 s, which means that the catalytic effect of Li₂CO₃ is very significant.

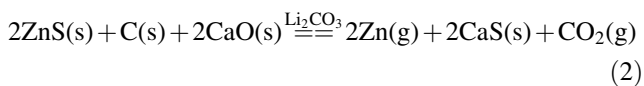
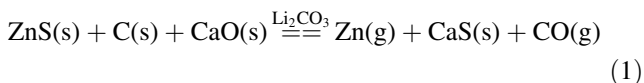
The other interesting observation from these two figures is that the amount of Li₂CO₃ almost remains unchanged with time or temperature. The reason is that it is a catalyst, the amount of which should not be varied.

According to the mechanism of Abramowitz and Rao [1], Na₂S and Na₂O are the intermediates for the Na₂CO₃-catalyzed reaction. Accordingly, in our system

(with Li₂CO₃ catalyst) Li₂S and Li₂O may be the intermediate products. The characteristic peaks for Li₂S and Li₂O were searched on the XRD patterns of partially reacted sample. Unfortunately, the existences of Li₂S and Li₂O can not be verified due to the overlaps of the peaks: those of Li₂S (2θ = 26.997° and 44.832°) with those of α-ZnS (2θ = 26.921°) and CaS (2θ = 44.997°); those of Li₂O (2θ = 33.612° and 56.373°) with those of ZnO (2θ = 34.438°), Li₂CO₃ (2θ = 34.107°) and α-ZnS (2θ = 56.399°).

Analysis of TGA and AAS

Lithium carbonate-catalyzed carbothermic reduction of zinc sulfide in the presence of calcium oxide may follow one of the following reactions.



Weight loss data obtained from TGA can be transformed to zinc yield, Y_{Zn}, according to Eq. 3 or Eq. 4

According to Reaction 1

$$Y_{\text{Zn}}(\%) = \frac{(W_o - W) / (MW_{\text{Zn}} + MW_{\text{CO}})}{N_{\text{ZnS}}^o} \times 100 \tag{3}$$

According to Reaction 2

$$Y_{\text{Zn}}(\%) = \frac{(W_o - W) / (2MW_{\text{Zn}} + MW_{\text{CO}_2})}{N_{\text{ZnS}}^o} \times 100 \tag{4}$$

where MW_{CO} is the molecular weight of CO, 38 kg kmol⁻¹; MW_{CO₂} the molecular weight of CO₂, 44 kg kmol⁻¹; MW_{Zn} the molecular weight of Zn, 65.39 kg kmol⁻¹; W the weight of solid sample at t = t, kg; W_o the weight of solid sample at t = 0, kg; N_{ZnS}^o the number of moles of ZnS in solid sample at t = 0, kmol.

Zinc yield, Y_{Zn}, at t = t can also be calculated from the data of AAS according to Eq. 5

$$Y_{\text{Zn}}(\%) = \frac{N_{\text{Zn}}^t - N_{\text{Zn}}^o}{N_{\text{Zn}}^o} \times 100 \tag{5}$$

where N_{Zn} is the number of moles of Zn in solid sample at t = t, kmol; N_{Zn}^o the number of moles of Zn in solid sample at t = 0, kmol.

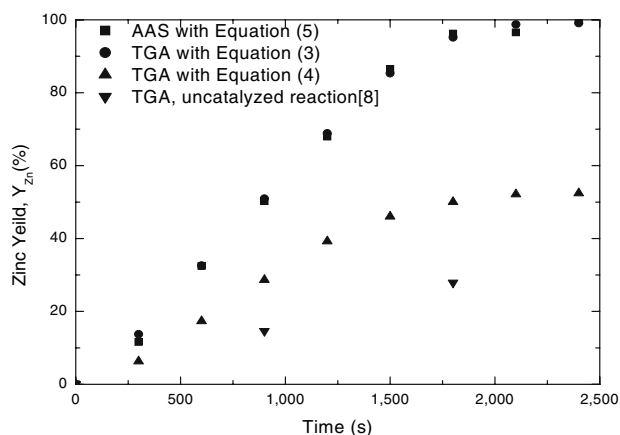


Fig. 3 Comparison of the results of TGA and AAS. Q, 0.50 × 10⁻⁵ m³ s⁻¹; h, 0.005 m; T, 1,303 K; N_C^o/N_{ZnS}^o, 2.0; N_{CaO}^o/N_{ZnS}^o, 1.5; N_{Li₂CO₃}^o/N_{ZnS}^o, 0.015; d_{ZnS}, 5.98 × 10⁻⁶ m; d_C, 67.7 × 10⁻⁶ m; d_{CaO}, 17.90 × 10⁻⁶ m; ρ_o, 429.1 kg m⁻³

The relationship between zinc yield, Y_{Zn}, and reaction time t according to Eqs. 3, 4 and 5 are plotted in Fig. 3. As can be seen, the results of TGA with Eq. 3 are very close to those of AAS, whereas those of TGA with Eq. 4 are not. This implies that the actual reaction follows Eq. 1. Also shown in this figure are the data of the uncatalyzed reaction [8]. After a close comparison of the results of catalyzed reaction of Reaction 1 and that of uncatalyzed reaction [8], one observes that the reaction can greatly be enhanced by adding Li₂CO₃ catalyst. The results obtained coincide with XRD results presented before.

Analysis of CSD, EA and TGA

The weight of carbon, W_C, in a solid sample can be calculated according to Reaction 1

$$W_C = W_{C_o} - \frac{(W_o - W) \times MW_C}{(MW_{\text{Zn}} + MW_{\text{CO}})} \tag{6}$$

or Reaction 2

$$W_C = W_{C_o} - \frac{(W_o - W) \times MW_C}{(2MW_{\text{Zn}} + MW_{\text{CO}_2})} \tag{7}$$

where W_C is the weight of carbon in solid sample at t = t, kg; W_{C_o} the weight of carbon in solid sample at t = 0, kg.

The weight of sulfur in a solid sample, however, remains constant, since it is scavenged in the solid during reaction.

The relationship between the weight of carbon and reaction times as well as that between weight of sulfur and reaction times at 1,303 K determined by CSD and EA as well as those deduced from the TGA results, or theoretical

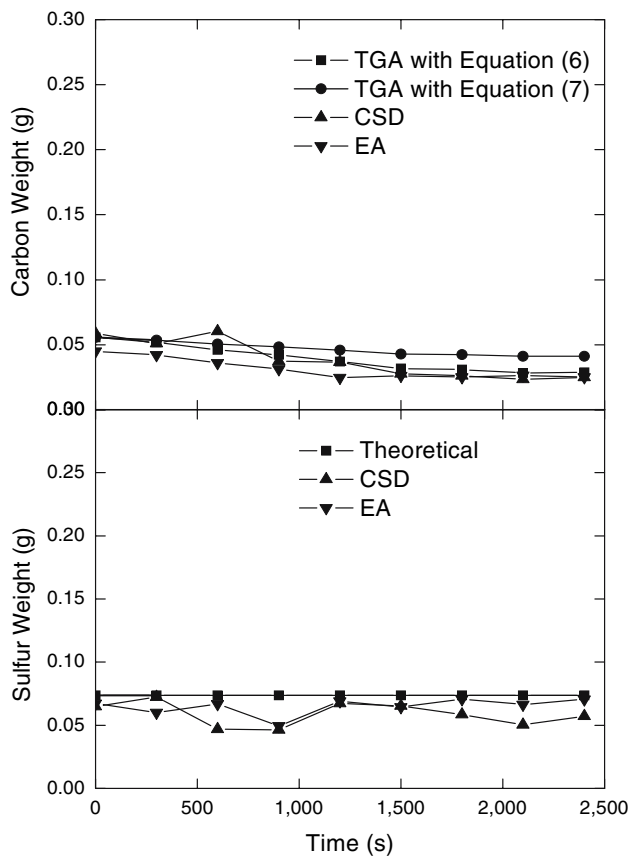


Fig. 4 Plot of total carbon and total sulfur of a partially reacted solid sample against reaction time. Q , $0.50 \times 10^{-5} \text{ m}^3 \text{ s}^{-1}$; h , 0.005 m; T , 1,303 K; $N_{\text{C}}^{\circ}/N_{\text{ZnS}}^{\circ}$, 2.0; $N_{\text{CaO}}^{\circ}/N_{\text{ZnS}}^{\circ}$, 1.5; $N_{\text{Li}_2\text{CO}_3}^{\circ}/N_{\text{ZnS}}^{\circ}$, 0.015; d_{ZnS} , 5.98×10^{-6} m; d_{C} , 67.7×10^{-6} m; d_{CaO} , 17.90×10^{-6} m; ρ_{o} , 429.1 kg m^{-3}

value, are depicted in Fig. 4, while the weights of carbon and sulfur in the solid sample for different reaction temperatures are shown in Fig. 5. Again, the TGA results calculated according to Eq. 6 are found to be closer to those of CSD and EA than those calculated according to Eq. 7. This finding is considered to lend support indirectly to the correctness of Reaction 1.

The weights of carbon and sulfur obtained from CSD and EA are found to be generally less than those obtained from TGA, or theoretical value. This is due to the slight oxidation of carbon and sulfur in the stage between removing and quenching the sample. Nevertheless, the agreements between the results of CSD, EA and TGA, or theoretical value, are fair.

It can be seen from Fig. 4 that the weight of carbon per sample reduces monotonically with time while that of sulfur remains unchanged. The reduction of carbon is caused by the evolution of carbon monoxide gas during reaction while the constant content of sulfur is attributed to the fact that sulfur is trapped as calcium sulfide in the solid sample.

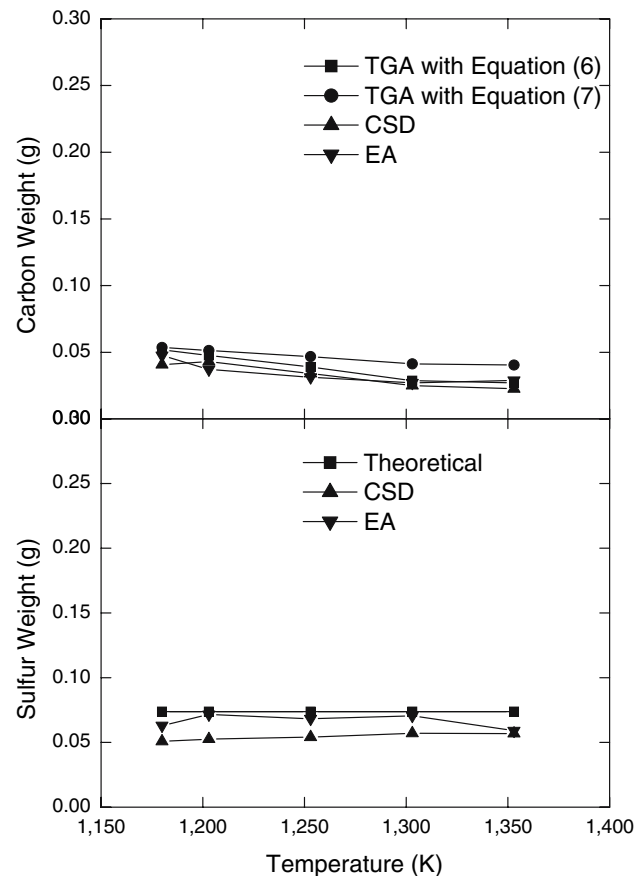


Fig. 5 Plot of total carbon and total sulfur of a partially reacted solid sample against reaction temperature. Q , $0.50 \times 10^{-5} \text{ m}^3 \text{ s}^{-1}$; h , 0.005 m; $N_{\text{C}}^{\circ}/N_{\text{ZnS}}^{\circ}$, 2.0; $N_{\text{CaO}}^{\circ}/N_{\text{ZnS}}^{\circ}$, 1.5; $N_{\text{Li}_2\text{CO}_3}^{\circ}/N_{\text{ZnS}}^{\circ}$, 0.015; d_{ZnS} , 5.98×10^{-6} m; d_{C} , 67.7×10^{-6} m; d_{CaO} , 17.90×10^{-6} m; ρ_{o} , 429.1 kg m^{-3} ; t , 2,400s

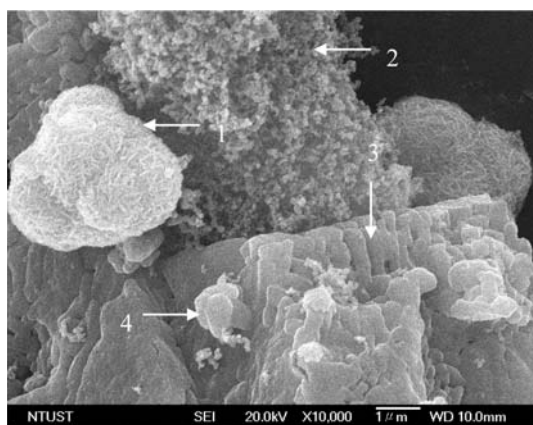
The effect of reaction temperature on the content of carbon and sulfur, shown in Fig. 5, is similar to that of reaction time. The low values of carbon content for the high temperatures are due to the high conversion of the reaction, while the constant sulfur content can be attributed to the fact that all sulfur is fixed in the solid sample.

The results obtained in this study agree qualitatively with those of Huang et al. [8].

Analysis of SEM

ZnS, C and CaO employed in this study are the same as those in our previous study and their scanning electron micrographs are shown there [8]. Li_2CO_3 , not used before, are found to be a rod or a granule with size in the range of 0.5×10^{-6} to 2.0×10^{-6} m [13].

Shown in Fig. 6a is the SEM picture taken from the unreacted sample. The grains of ZnS, C and CaO, represented by 1, 2 and 3, respectively, can be easily distinguished by their shapes and sizes. The



(a) 0 s



(b) 300 s

Fig. 6 Scanning electronmicrographs of solid samples. (a) 0 s and (b) 300 s. These micrographs were recorded using secondary electrons. 1: Zinc containing grain; 2: Carbon grain; 3: Calcium containing grain; 4: Lithium carbonate. Q , $0.50 \times 10^{-5} \text{ m}^3 \text{ s}^{-1}$; h , 0.005 m; T , 1,303 K; $N_{\text{C}}^0/N_{\text{ZnS}}^0$, 2.0; $N_{\text{CaO}}^0/N_{\text{ZnS}}^0$, 1.5; $N_{\text{Li}_2\text{CO}_3}^0/N_{\text{ZnS}}^0$, 0.015; d_{ZnS} , 5.98×10^{-6} m; d_{C} , 67.7×10^{-6} m; d_{CaO} , 17.90×10^{-6} m; ρ_o , 429.1 kg m^{-3}

Li_2CO_3 grain, represented by 4, however, is not quite certain. The SEM picture shown in Fig. 6b is taken from the solid sample reacted for 300 s. The findings from the SEM pictures taken in the catalyzed reaction system are similar to those of the uncatalyzed reaction [8].

The effects of temperature on the morphologies of zinc-containing, carbon and calcium-containing grains are similar to those of the uncatalyzed system [8].

Analysis of SAA

Specific surface areas, specific pore volumes and average pore diameters of one solid sample for different reaction times have been measured and the results are described below. The specific surface area was found to be reduced

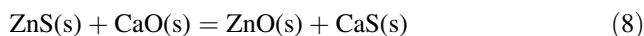
abruptly initially and then leveled off. The specific pore volume increased initially, reached maximum at 300 s, and then dropped until 800 s. After that, it leveled off. The average pore diameter, however, was observed to be similar to the variation in total surface area.

To explain the variations of these physical properties, the effects of following ‘‘changes’’ should be taken into account: phase transformation and decomposition of Li_2CO_3 , phase transformation of ZnS , zinc vapor evolution, carbon gasification, volume expansion of CaS and sintering of the solid sample. This seems to be a tough task. Therefore, the analysis of the results will not be given here.

The effects of reaction temperature and time on the variations in these physical properties are found to be similar.

Results of auxiliary experiments

The possible reaction between zinc sulfide and calcium oxide is



The extents of this reaction in the Li_2CO_3 catalyzed system and uncatalyzed system can be qualitatively known through the intensities of the characteristic peak of ZnO . A comparison of these peaks heights indicated that Li_2CO_3 was a good catalyst for the reaction between zinc sulfide and calcium oxide.

The XRD patterns of the solid samples before and after reaction for the second series of auxiliary experiments reaction between zinc sulfide and lithium carbonate are shown in Fig. 7. The results revealed that the peaks intensities of both β - ZnS and Li_2CO_3 are reduced, while that of α - ZnS is increased. The reduction in β - ZnS and increase in α - ZnS are due to its phase transformation of ZnS (from β type to α type), while the reduction in Li_2CO_3 is attributed to its partial decomposition [14]. Peaks of ZnO and Li_2S are not found in this XRD pattern. These results imply that no reaction takes place between zinc sulfide and lithium carbonate.

Reaction mechanism

Mechanism of lithium carbonate-catalyzed carbothermic reduction of zinc sulfide in the presence of calcium oxide has not been reported before. However, two mechanisms for sodium carbonate-catalyzed reaction have been proposed. The first one was proposed by Abramowitz and Rao [1], who presumed that reactions

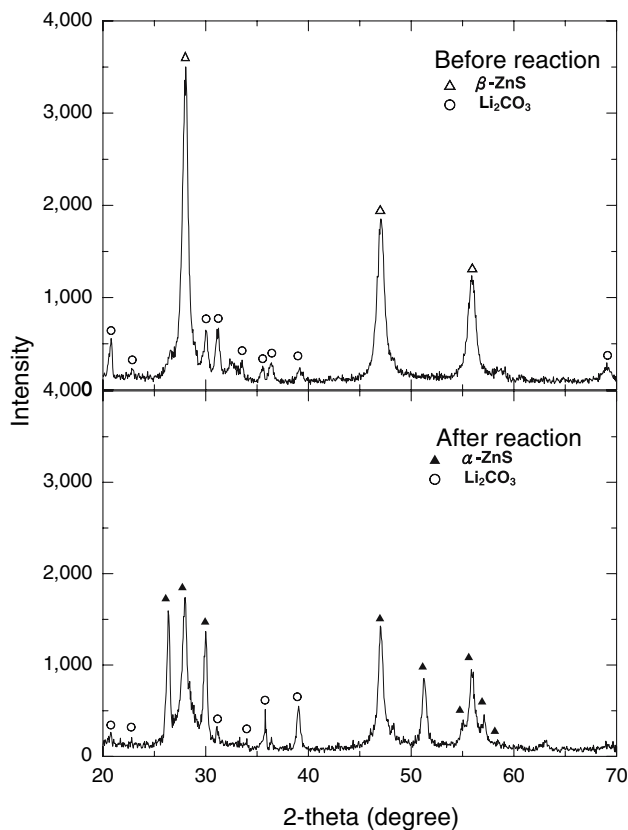
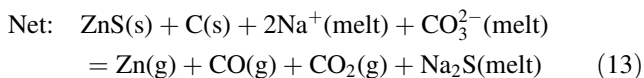
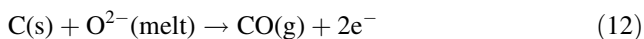
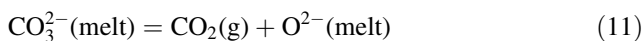
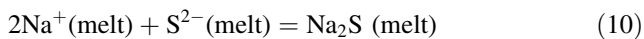
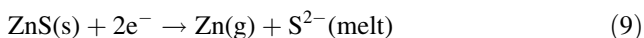


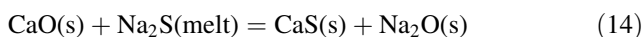
Fig. 7 X-ray diffraction patterns of solid samples before and after reaction between ZnS and Li_2CO_3 . Q , $0.50 \times 10^{-5} \text{ m}^3 \text{ s}^{-1}$; h , 0.005 m ; T , $1,303 \text{ K}$; t , $2,400 \text{ s}$; $N_{\text{Li}_2\text{CO}_3}^0/N_{\text{ZnS}}^0$, 1 ; d_{ZnS} , $5.98 \times 10^{-6} \text{ m}$

took place in the three regions of the sample: micro-pools of carbonate melt, melt/lime interface and melt/gas interface.

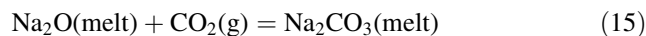
Micro-pools of carbonate melt:



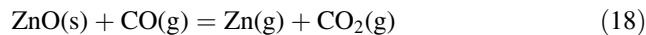
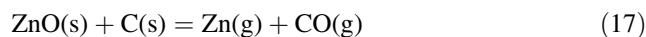
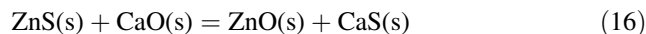
Melt/lime interface:



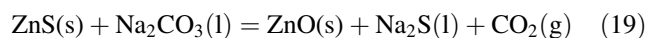
Melt/gas interface:



The second mechanism [4] retained the original reaction steps of non-catalyzed reactions:

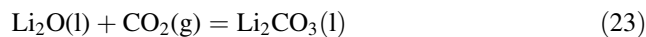
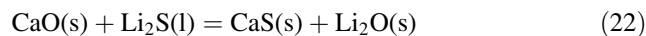
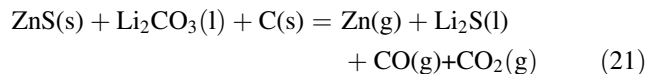


When Na_2CO_3 was added in the sample, the overall reaction was speeded up through the enhanced production rate of ZnO, which is achieved by the catalytic effect of molten Na_2CO_3 on Reaction 16 or according to Eq. 19



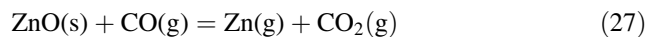
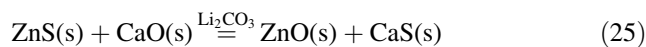
Since lithium and sodium are alike, the mechanism for lithium carbonate-catalyzed reaction and that for sodium carbonate-catalyzed reaction may be similar. The first possible mechanism for $\text{ZnS/C/CaO/Li}_2\text{CO}_3$ is adopted from Abramowitz and Rao [1].

First mechanism



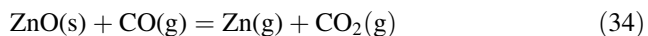
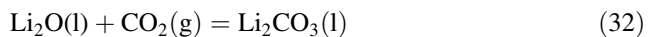
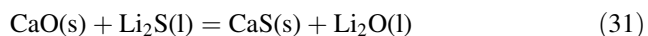
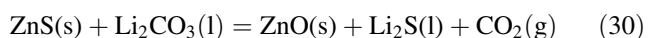
The second and third mechanisms are derived from the proposition of Ueda et al. [4].

Second mechanism



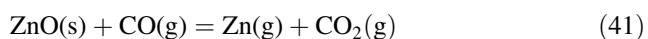
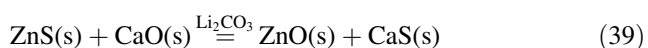
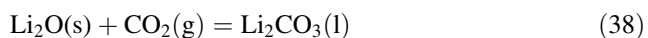
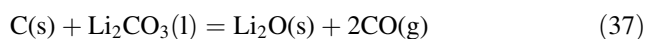
Third mechanism





The fourth possible mechanism is derived from the possible reaction between C(s) and Li₂CO₃(l), which were found by Kim and Lee [14].

Fourth mechanism



The observation of the intermediate product of ZnO in our XRD analysis (Fig. 1) helps us exclude the possibility of the first mechanism, since ZnO is not an intermediate product in this mechanism. The calculated standard Gibbs free energy change for Reaction 30 at 1,303 K, 66.83 kJ mol⁻¹ [15], implies that this reaction is not a spontaneous one. Furthermore, it has been proved in auxiliary experiments that the reaction between ZnS(s) and Li₂CO₃ (l) is impossible. Consequently, the third mechanism is ruled out.

The results of the first series of auxiliary experiments shown before support the catalytic effect of molten Li₂CO₃ on the reaction between zinc sulfide and calcium oxide, Reaction 25 or 39. Therefore, both the second and fourth mechanisms are possible. Examining these two mechanisms reveals that the fourth mechanism contains all the reaction steps of the second one. Moreover, Reactions 37 and 38 in the fourth mechanism explain the reaction cycle

of Li₂CO₃ catalyst. Hence, the fourth mechanism, Reactions 36–42, is considered to be the mechanism of this reaction system. It should be emphasized again that the catalytic effect of Li₂CO₃ is two-fold. One is the generation of more CO through Reaction 37 and the other is the production of more ZnO due to the catalytic effect of molten Li₂CO₃ through Reaction 39.

Conclusions

1. Carbothermic reduction of ZnS in the presence of CaO is found to be greatly enhanced by molten Li₂CO₃.
2. The results of TGA are found to be close to those of AAS while the agreements between the results of TGA, CSD and EA are found to be fair.
3. A reaction mechanism is proposed to interpret the overall reaction.

Acknowledgements The authors are grateful to the National Science Council of Taiwan for the financial support (NSC93-2214-E-011-012).

References

1. Abramowitz H, Rao YK (1978) *Trans Inst Min Metall (Sec C)* 87:180
2. Hsu HC, Lin CI, Chen HK (2004) *Metall Mater Trans B* 35:55
3. Skopov GV, Kharitidi GP, Tikhonov AI (1976) *Izv Vyssh Ucheb Zaved, Tsvet Metall* 4:33; *Chem Abstr* (1976)85:146312
4. Ueda Y, Nakamura T, Noguchi F (1983) *J Min Met Japan* 99:127
5. Zhang C, Asakura I, Ogawa O (1988) *J Min Met Japan* 104:469
6. Zhang C, Asakura I, Ogawa O (1988) *J Min Met Japan* 104:837
7. Zhang C, Shimpo R, Asakura I, Ogawa O (1989) *J Min Mat Proc Inst Japan* 105:475
8. Huang CH, Lin CI, Chen HK (2005) *J of Mat Sci* 40:4299
9. Wu CM (2004) MS Thesis, Department of Chemical Engineering, National Taiwan University of Science and Technology, Taipei, Taiwan
10. Brunauer S, Emmett P, Teller E (1983) *J Amer Chem Soc* 60:309
11. Barret EP, Joyner LG, Halenda PP (1951) *J Amer Chem Soc* 73:373
12. Joint Committee On Powder Diffraction Standards, *Powder Diffraction File.*, Card 4-836, Card 5-492, Card 5-664, Card 5-586, Card 8-464, Card 37-1497, Card 22-1141, International Center for Diffraction Data, Swarthmore, PA 1990
13. Peng YC (2005) MS Thesis, National Taiwan University of Science and Technology, Taipei, Taiwan
14. Kim JW, Lee HG (2001) *Metall Mater Trans B* 32:17
15. Kubaschewski O, Evans EL, Alcock CB (1993) *Metallurgical thermochemistry*. Pergamon Press, Oxford, United Kingdom